Three novel MOFs constructed from 1,3,5-tris(1-imidazolyl)benzene and dicarboxylate ligands and the selective adsorption for C_2H_2/C_2H_4 and C_2H_6/CH_4

Ming-Xing Yang, Li-Juan Chen, Jing Gao, Yang Gao, Guang-Tao Yu* and Shen Lin*

College of Chemistry and Materials Science, Fujian Provincial Key Laboratory of Advanced Materials Oriented Chemical Engineering, Engineering Research Center of Industrial Biocatalysis, Fujian Province Higher Education Institutes, Fujian Normal University, Fuzhou, Fujian 350007, People's Republic of China

Contents

1. Structure analyses and table of crystallographic data.

2. IR spectrum, TGA and PXRD

3. Gas adsorption isotherms and pore size distribution

4. Calculation of sorption heat

5. Prediction of the gas adsorption selectivity by IAST.

6. Computational methods.

1. Structure analyses and table of crystallographic data.

The structure analysis was performed with direct methods using SHELXS-2018/3. A multi-scan absorption was applied to the intensity data. Structure refinement was done against *F*2 using SHELXL-2018/3. All nonhydrogen atoms were refined with anisotropic displacement parameters. The highly disordered solvent molecules of compounds are removed using the *SQUEEZE* routine of the *PLATON*. The final formulas of compounds were determined by crystal structure analysis combined with elemental analyses and TG.

Table S1 Crystallographic data

Compound	1	2	3
Empirical formula	$Co_3C_{53}H_{46}N_{16}O_{14}$	$Co_3C_{46}H_{56}N_{14}O_{14}$	$Zn_3C_{64}H_{60}I_2N_{16}O_{12}$
Formula weight	1307.85	1205.83	1695.19
Crystal system	Monoclinic	Triclinic	Triclinic
Space group	C2/c	P-1	P-1
a(Å)	27.9125(15)	11.0686(4)	11.6710(18)
b(Å)	26.8494(13)	15.4778(4)	15.111(2)
c(Å)	10.1473(5)	17.4148(2)	20.142(3)
α(°)	90	64.292(4)	88.674(4)
β(°)	97.654(4)	81.548(7)	75.755(3)
γ(°)	90	89.247(7)	79.393(5)
V(Å^3)	7537.0(7)	2654.66(15)	3383.3(9)
Z	4	2	2
F(000)	2676	1246	1696
D_{calcd}(g·cm^{-3})	1.153	1.509	1.664
μ(mm^{-1})	0.713	1.004	2.040
θ_{max}, θ_{min} (°)	27.480,2.114	27.469, 2.281	27.500, 2.127
R_{int}	0.0341	0.0356	0.0261
No. of data collected	29764	30570	39765
No. of unique data	8584	11988	15379
No. of observed	7891	10486	13043
No. variables	368	534	786
Final R indicaes [I>2σ(I)]	R_1 = 0.0443, wR_2 = 0.1096	R_1 = 0.0552, wR_2 = 0.1696	R_1 = 0.0349, wR_2 = 0.0934
R indices(all data)	R_1 = 0.0485, wR_2 = 0.1125	R_1 = 0.0614, wR_2 = 0.1758	R_1 = 0.0421, wR_2 = 0.0986
Goof	1.033	1.029	1.010
(Δ/σ)max,mean	0.001,0.000	0.001,0.000	0.003,0.000
$\Delta\rho_{max}$ /$\Delta\rho_{min}$ (e/ Å^3)	0.361/-0.393	1.464/-0.853	1.008/-0.884

[a] $R_1 = \sum \| F_o | - | F_c \| / \sum | F_o |$, $wR = \{\sum[w(F_o^2 - F_c^2)^2] / [\sum w(F_o^2)^2]\}^{1/2}$

Table S2 Selected bond lengths(Å)and bond angles(º)of compound 1

Co(1)-O(2A)	2.0212(15)	Co(1)-O(1)	2.0322(15)	Co(1)-O(5)	2.0972(14)
Co(1)-O(6B)	2.1319(15)	Co(1)-N(1)	2.1497(17)	Co(1)-N(3C)	2.1517(17)
Co(2)-N(6D)	2.0652(16)	Co(2)-N(6E)	2.0652(16)	Co(2)-O(3F)	2.0862(14)
Co(2)-O(3)	2.0862(14)	Co(2)-O(4F)	2.2564(14)	Co(2)-O(4)	2.2564(14)

O(2A)-Co(1)-O(1)	101.44(6)	O(2A)-Co(1)-O(5)	164.10(6)
O(1)-Co(1)-O(5)	94.31(6)	O(2A)-Co(1)-O(6B)	85.09(6)
O(1)-Co(1)-O(6B)	171.93(6)	O(5)-Co(1)-O(6B)	79.04(5)
O(2A)-Co(1)-N(1)	94.03(7)	O(1)-Co(1)-N(1)	92.04(7)
O(5)-Co(1)-N(1)	87.52(6)	O(6B)-Co(1)-N(1)	92.22(6)
O(2A)-Co(1)-N(3C)	89.25(7)	O(1)-Co(1)-N(3C)	87.50(7)
O(5)-Co(1)-N(3C)	89.27(6)	O(6B)-Co(1)-N(3C)	87.86(7)
N(1)-Co(1)-N(3C)	176.72(7)	N(6D)-Co(2)-N(6E)	102.89(9)
N(6D)-Co(2)-O(3F)	102.82(6)	N(6E)-Co(2)-O(3F)	94.39(6)
N(6D)-Co(2)-O(3)	94.39(6)	N(6E)-Co(2)-O(3)	102.82(6)
O(3F)-Co(2)-O(3)	152.30(9)	N(6D)-Co(2)-O(4F)	86.36(6)
N(6E)-Co(2)-O(4F)	154.60(6)	O(3F)-Co(2)-O(4F)	60.32(5)
O(3)-Co(2)-O(4F)	99.94(6)	N(6D)-Co(2)-O(4)	154.60(6)
N(6E)-Co(2)-O(4)	86.36(6)	O(3F)-Co(2)-O(4)	99.94(6)
O(3)-Co(2)-O(4)	60.32(5)	O(4F)-Co(2)-O(4)	95.29(8)

Symmetry Code: A, -x+1/2,-y+1/2,-z+1; B,-x+1/2,-y+1/2,-z; C,-x+1/2,y+1/2,-z+1/2; D, -x,y,-z+1/2; E, x,y,z+1; F, -x,y,-z+3/2 .

Table S3 Selected bond lengths(Å)and bond angles(º)of compound 2

Co(1)-O(2)	2.060(2)	Co(1)-O(6)	2.061(2)	Co(1)-O(9)	2.1027(19)
Co(1)-N(3)	2.125(3)	Co(1)-O(4A)	2.192(2)	Co(1)-N(1B)	2.229(3)
Co(2)-O(1)	2.070(2)	Co(2)-O(10)	2.090(2)	Co(2)-O(5)	2.096(2)
Co(2)-O(8C)	2.122(2)	Co(2)-O(9)	2.128(2)	Co(2)-N(8B)	2.153(3)
Co(3)-O(9)	1.9717(19)	Co(3)-O(3)	1.978(2)	Co(3)-O(7C)	1.994(2)
Co(3)-N(6D)	2.054(3)				

O(2)-Co(1)-O(6)	108.73(11)	O(2)-Co(1)-O(9)	98.27(8)
O(6)-Co(1)-O(9)	83.92(10)	O(2)-Co(1)-N(3)	88.35(9)
O(6)-Co(1)-N(3)	88.47(11)	O(9)-Co(1)-N(3)	171.20(9)
O(2)-Co(1)-O(4A)	163.09(9)	O(6)-Co(1)-O(4A)	86.96(10)
O(9)-Co(1)-O(4A)	89.42(8)	N(3)-Co(1)-O(4A)	85.74(10)
O(2)-Co(1)-N(1B)	85.77(9)	O(6)-Co(1)-N(1B)	164.32(12)
O(9)-Co(1)-N(1B)	88.18(8)	N(3)-Co(1)-N(1B)	98.14(9)
O(4A)-Co(1)-N(1)	79.41(9)	O(1)-Co(2)-O(10)	88.04(10)
O(1)-Co(2)-O(5)	97.39(9)	O(10)-Co(2)-O(5)	87.53(10)
O(1)-Co(2)-O(8C)	173.05(9)	O(10)-Co(2)-O(8C)	91.36(11)
O(5)-Co(2)-O(8C)	89.50(9)	O(1)-Co(2)-O(9)	92.71(8)
O(10)-Co(2)-O(9)	178.93(9)	O(5)-Co(2)-O(9)	91.61(8)

O(8C)-Co(2)-O(9)	87.99(9)	O(1)-Co(2)-N(8B)	86.06(10)
O(10)-Co(2)-N(8B)	90.96(11)	O(5)-Co(2)-N(8B)	176.18(9)
O(8C)-Co(2)-N(8B)	87.02(9)	O(9)-Co(2)-N(8B)	89.86(10)
O(9)-Co(3)-O(3A)	124.39(8)	O(9)-Co(3)-O(7C)	119.39(9)
O(3A)-Co(3)-O(7C)	104.32(9)	O(9)-Co(3)-N(6D)	105.45(10)
O(3A)-Co(3)-N(6D)	100.28(10)	O(7C)-Co(3)-N(6D)	97.98(10)

Symmetry Code: A, x+1,y,z; B, -x,-y,-z+1; C, -x+1,-y+1,-z; D, x,y+1,z;

Table S4 Selected bond lengths(Å)and bond angles(°)of compound 3

I(1)-Zn(1)	2.5527(5)	I(2)-Zn(3)	2.5267(5)	Zn(1)-O(1)	1.951(2)
Zn(1)-O(2)	2.959(2)	Zn(1)-N(1)	2.002(2)	Zn(1)-N(4A)	2.031(2)
Zn(2)-O(4B)	1.9565(18)	Zn(2)-O(5)	2.563(2)	Zn(2)-O(6)	1.981(2)
Zn(2)-N(6)	2.022(2)	Zn(2)-N(7)	2.0247(19)	Zn(3)-O(8C)	1.9696(18)
Zn(3)-N(12)	2.007(2)	Zn(3)-N(9D)	2.029(2)	Zn(3)-O(7C)	2.816(2)

O(1)-Zn(1)-N(1)	116.31(10)	O(1)-Zn(1)-N(4A)	103.60(9)
N(1)-Zn(1)-N(4A)	105.49(9)	O(1)-Zn(1)-I(1)	111.06(7)
N(1)-Zn(1)-I(1)	109.90(6)	N(4A)-Zn(1)-I(1)	110.04(6)
O(4B)-Zn(2)-O(6)	107.87(10)	O(4B)-Zn(2)-N(6)	107.54(8)
O(6)-Zn(2)-N(6)	124.79(11)	O(4B)-Zn(2)-N(7)	123.73(8)
O(6)-Zn(2)-N(7)	94.21(9)	N(6)-Zn(2)-N(7)	99.75(8)
O(8C)-Zn(3)-N(12)	116.22(9)	O(8C)-Zn(3)-N(9D)	95.40(8)
N(12)-Zn(3)-N(9D)	107.58(9)	O(8C)-Zn(3)-I(2)	115.97(7)
N(12)-Zn(3)-I(2)	109.90(7)	N(9D)-Zn(3)-I(2)	110.50(6)

Symmetry Code: A , -x-1,-y+1,-z+2; B , -x-1,-y,-z+2; C, x+1,y,z-1; D, x+1,y,z;

2. PXRD, IR spectrum and TGA

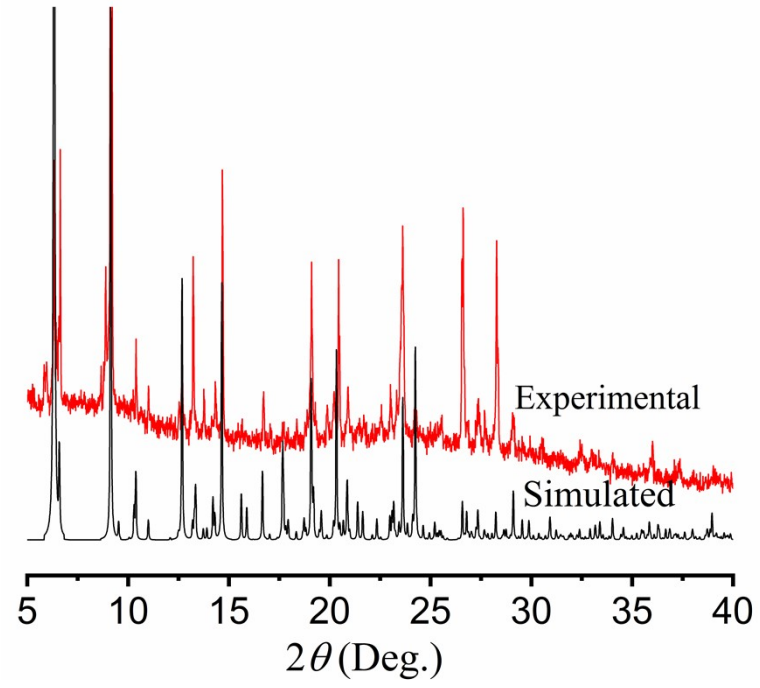

(a)

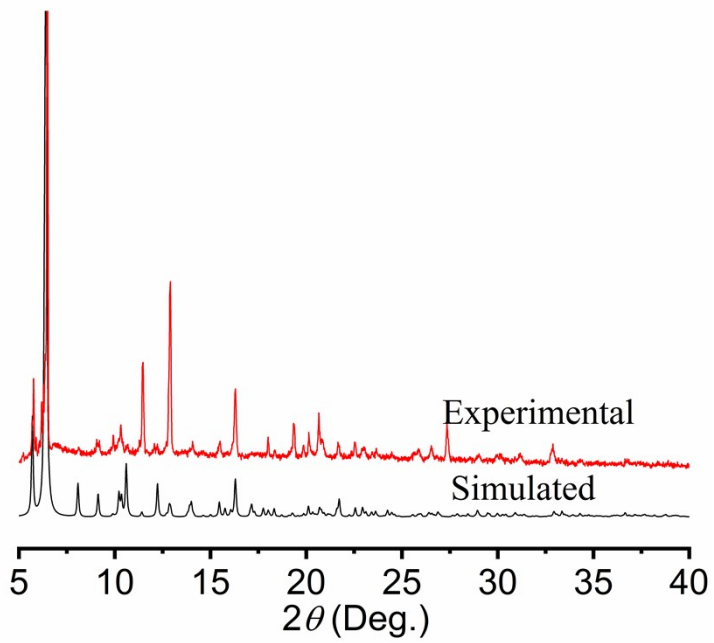

(b)

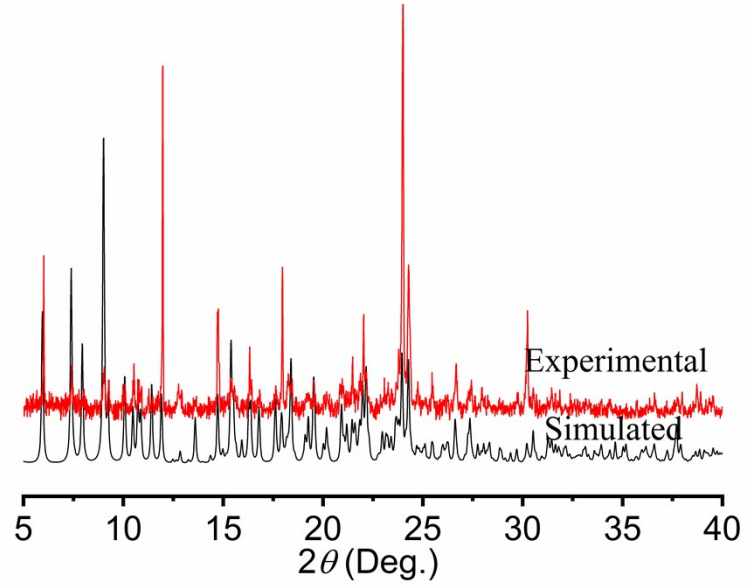

(c)

Fig. S1 Experimental X-ray powder pattern and simulated powder pattern based on the results from single-crystal X-ray diffraction for compounds 1(a),2(b),3(c)

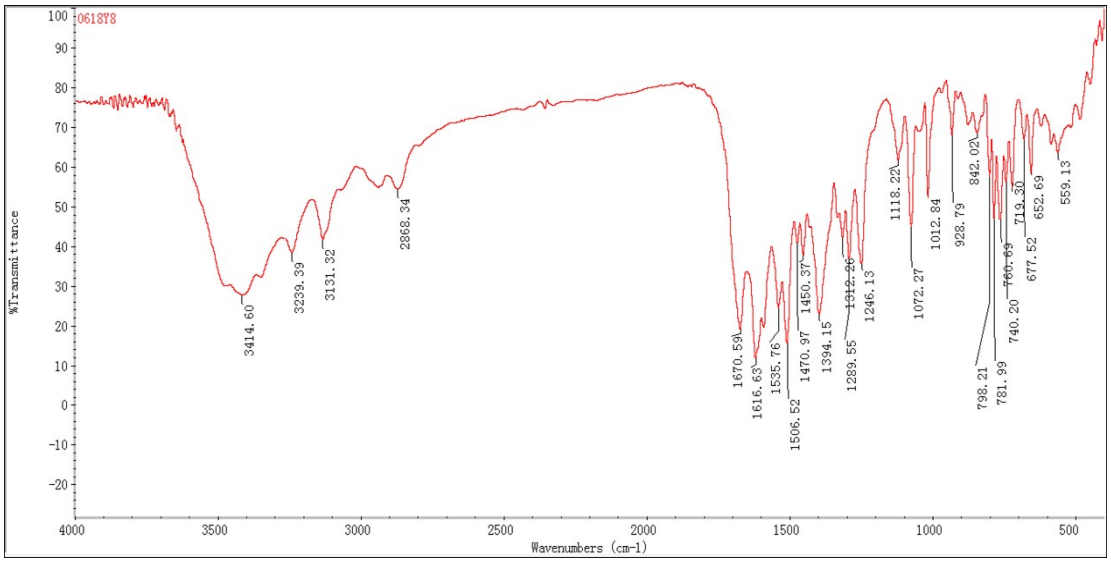

Figure.S2. IR of compound 1

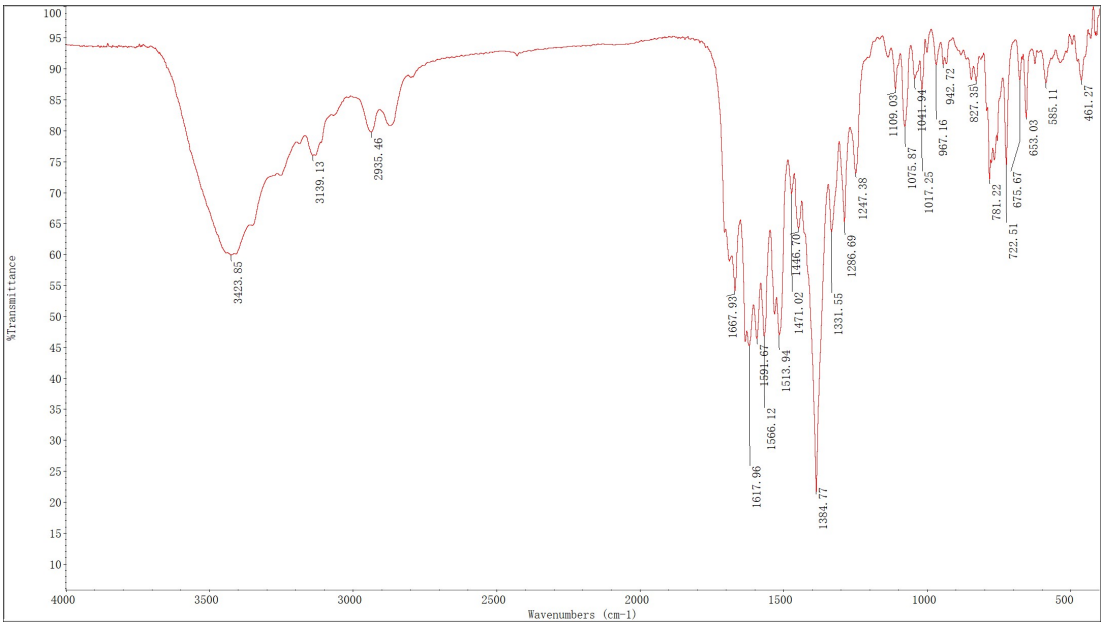

Figure.S3. IR of compound 2

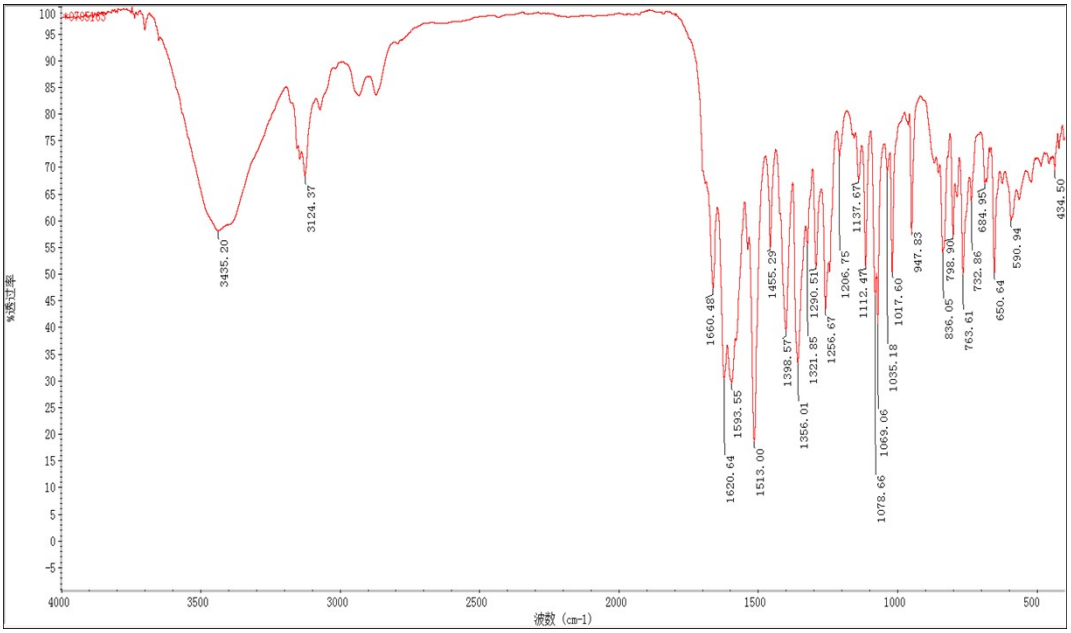

Figure.S4. IR of compound 3

The analyses of IR spectra

The observed peaks in the range of 3414 to 3435 cm^{-1} in FT-IR spectrum of 1-3 are attributed to O–H, N-H stretching vibration of H_2O or $–NH_2$[1]. The bands at ca. 3124–3139 are related to the C–H of benzene ring[2] and the peaks at 1506–1591 cm^{-1} are assigned to C=C(C=N) stretching vibrations of the imidazole and benzene ring[3-4]. The peaks around 1384–1398 and 1616-1620 cm^{-1} correspond to C=O asymmetric and symmetric stretching vibrations of the coordinated carboxylate group, respectively[2, 5-6]. And the C=O out-of-phase stretching bands are clearly observed in the approximately 1660–1670 cm^{-1} region with weak intensity as reported by the literature[3]. The C–O stretching vibrations of coordinated carboxylate group are observed at 1266-1290 cm^{-1} [3, 7] The absence of bands ranging from 1690 to 1710 cm^{-1} in 1-3 shows the complete deprotonation of carboxylic groups, in good agreement with the results of the structure analysis[8]. Characteristic frequency of the NH_2 group appeared at 1246 /1247cm^{-1} in 1 and 2 is attributed to the twisting modes[9]. The observed infrared spectra at 677/675 cm^{-1} in 1 and 2 correspond to the NH_2 wagging modes[9], the C-H of the ring out of plane bending modes of C-H is at 653-650/719-732 cm^{-1}[9]. The bands in the range of 1017–1078 cm^{-1} are caused by the stretching vibrations of C-N and the in-plane bending vibration of C-H in aromatic ring[4]. The bands observed at 400–590 cm^{-1} are assigned to the Co–O or Zn–O stretching vibrations[2].

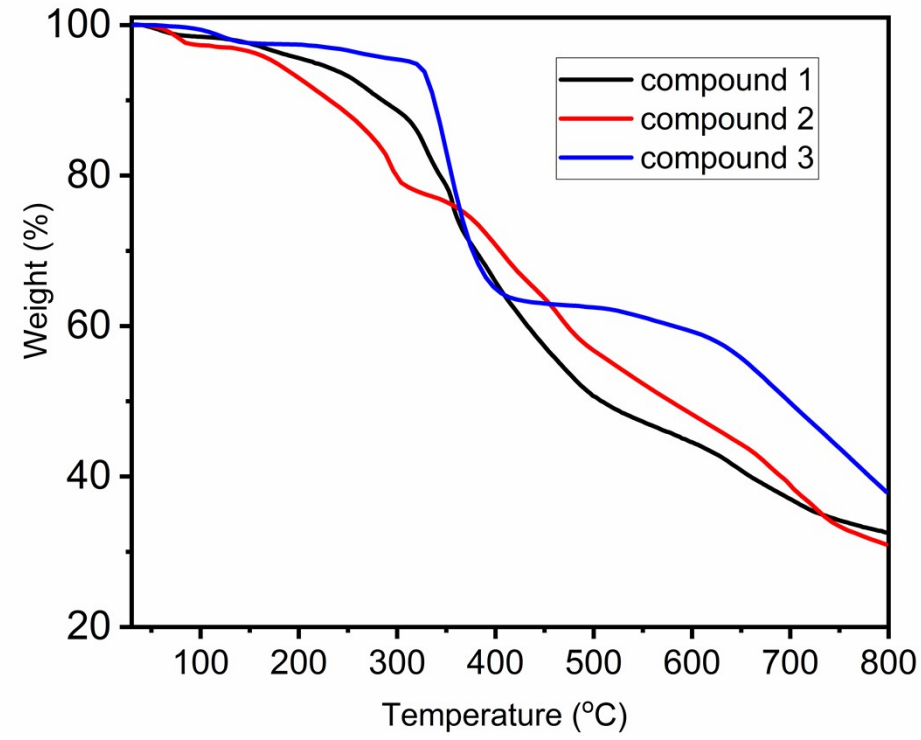

Fig. S5 The TG curve of compounds 1-3 under N_2 atmosphere at a heating rate of 10 K·min^{-1}.

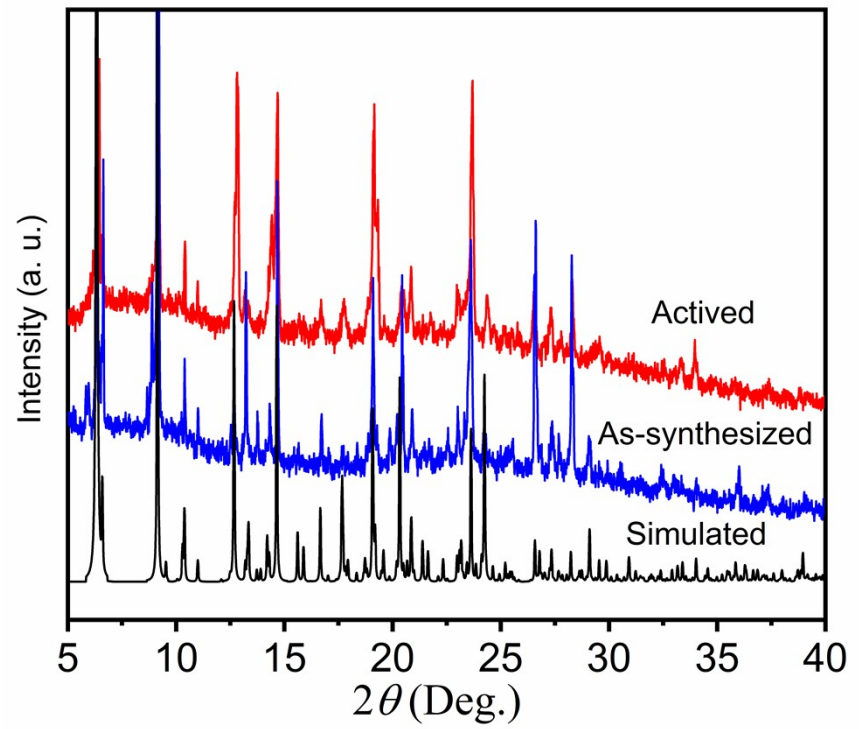

Fig. S6 Powder X-ray diffraction (PXRD) patterns for compound 1.

3. Gas adsorption isotherms and pore size distribution

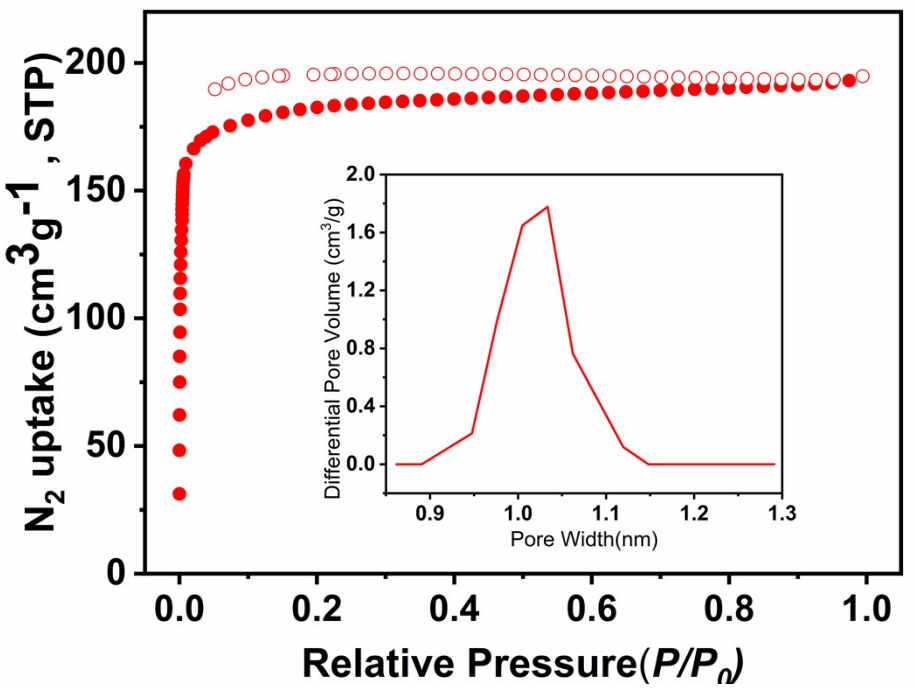

Fig. S7 N_2 adsorption and desorption isotherms for the active compound 1 at 77K. (Inset: the pore-size distribution from N_2 adsorption at 77 K (calculated by the non-local density functional theory)).

4. Calculation of sorption heat

$$\ln(p) = \ln(N) + (\frac{1}{T})\sum_{i=0}^{m} a_i \times N^i + \sum_{j=0}^{n} b_j \times N^j \qquad Q_{st} = -R \times \sum_{i=0}^{m} a_i \times N^i$$

The above virial expression was used to fit the combined isotherm data for 1 at 273 and 296 K, where P is the pressure, N is the adsorbed amount, T is the temperature, a_i and b_j are virial coefficients, and m and N are the number of coefficients used to describe the isotherms. Q_{st} is the coverage-dependent enthalpy of adsorption and R is the universal gas constant.

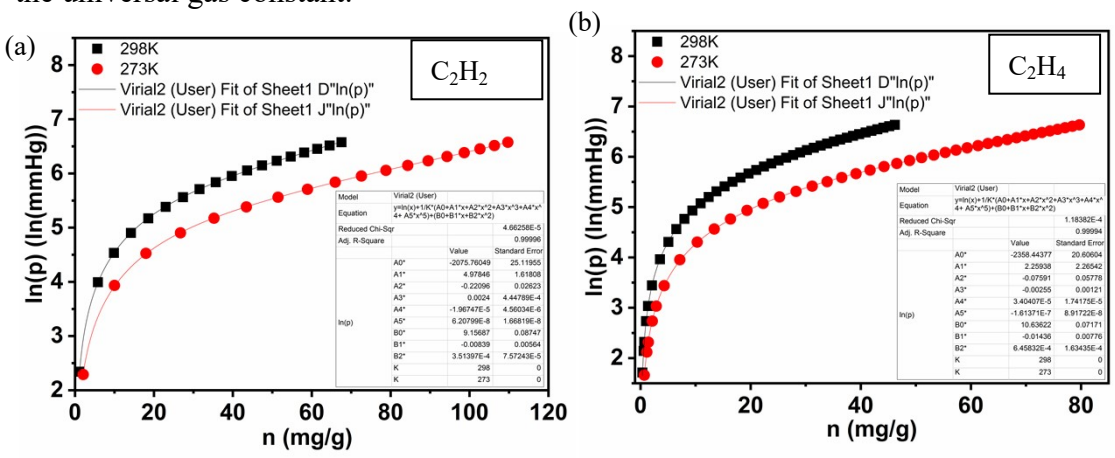

Fig.S8 The virial graphs for adsorption of C_2H_2(a)、C_2H_4(b) on compound 1

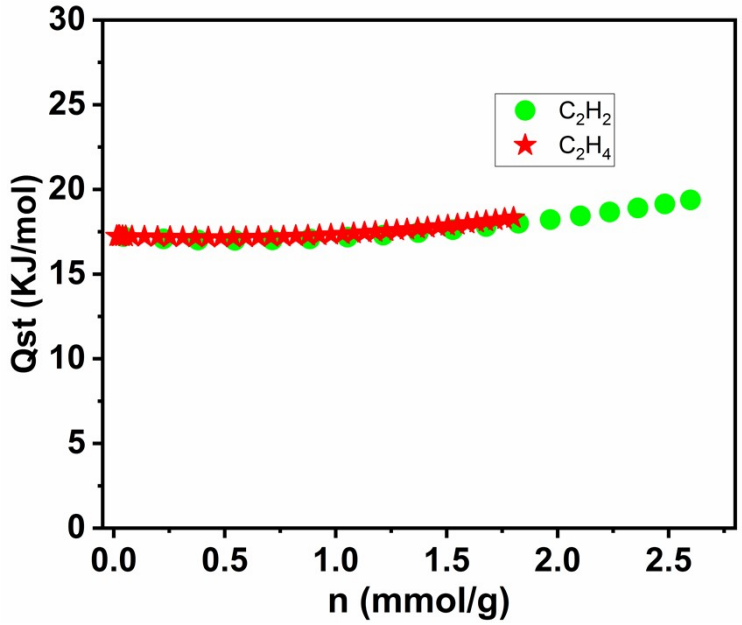

Fig.S9 The enthalpies for gas adsorption of C_2H_4 and C_2H_2 on compound 1

5. Prediction of the Gas Adsorption Selectivity by IAST.

The ideal adsorption solution theory (IAST) was used to predict the binary mixture adsorption from the experimental pure gas isotherms. To perform the integrations required by IAST, single-component isotherms should be fitted by the correct model. In practice, several methods are available; for this set of data we found that the single site. Langmuir-Freundlich equation was successful in fitting the results.

$$N = N^{\max} \times \frac{bp^{1/2}}{1 + bp^{1/n}}$$

where P is the pressure of the bulk gas in equilibrium with the adsorbed phase (kPa), N is the amount adsorbed per mass of adsorbent (mmol g^{-1}), Nmax is the saturation capacities of site 1 (mmol g^{-1}), b is the affinity coefficients of site 1 (1/kPa) and n represents the deviations from an ideal homogeneous surface. The fitted parameters were then used to predict multi-component adsorption with IAST. The adsorption selectivities based on IAST for mixed C_2H_2/C_2H_6、C_2H_2/CH_4、C_2H_4/C_2H_6 and C_2H_4/CH_4 are defined by the following equation:

$$S_{A/B} = (x_A/y_A)/(x_B/y_B)$$

where x_i and y_i are the mole fractions of component i (i = A, B) in the adsorbed and

bulk phases, respectively.

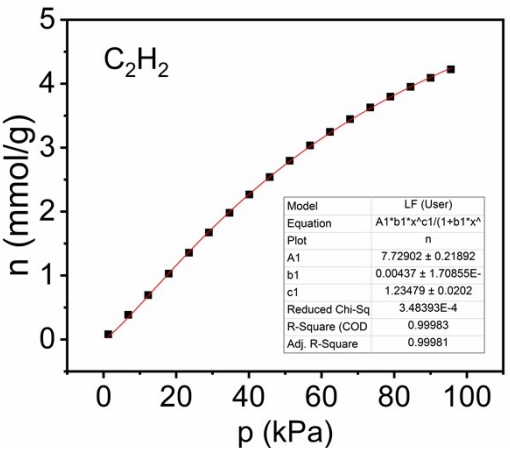

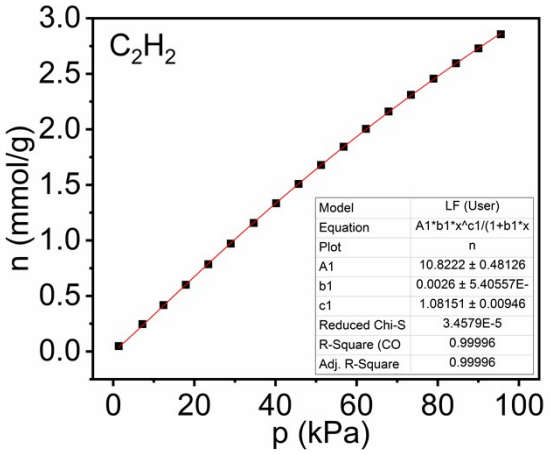

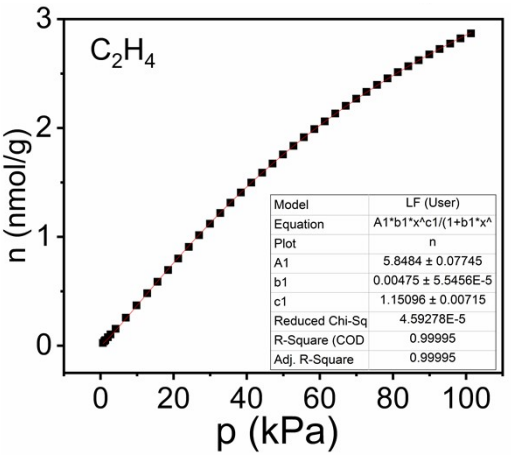

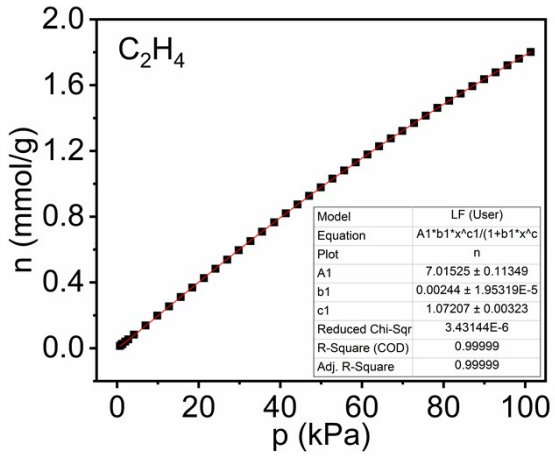

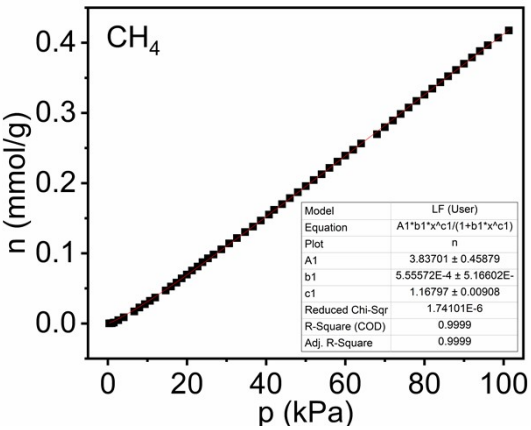

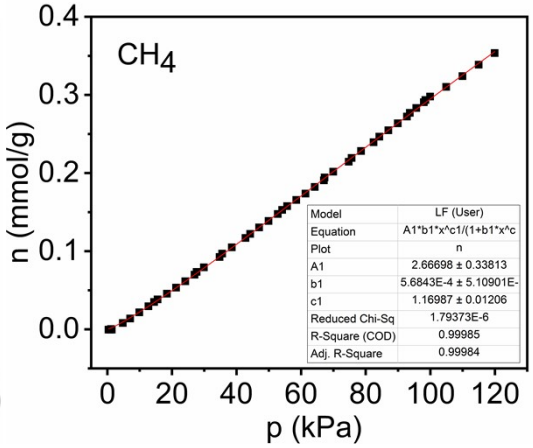

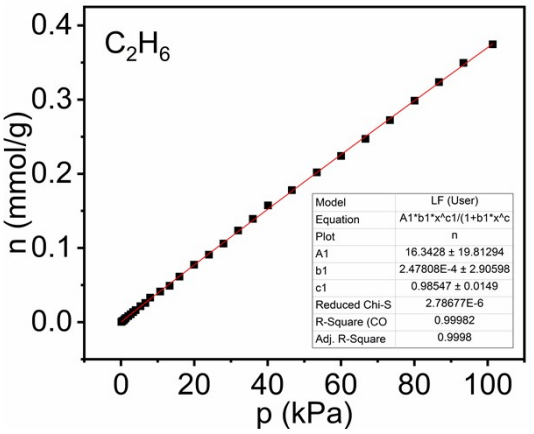

Fig.S10 The graphs of the single-site Langmuir-Freundlich equations fits for adsorption of C_2H_4, C_2H_2, CH_4 and C_2H_6 on compound 1 at 273K (left) and 296K (right).

6. Computational methods.

In this work, the generalized gradient approximation (GGA) with the Perdew–Burke–Ernzerh (PBE)[10] of the exchange correlation functional (including a semi-empirical van der Waals (vdW)[11] correction to account for the dispersion interactions) and a 400 eV cut off for the plane-wave basis set are adopted to perform all the density functional theory (DFT)[12] computations of the studied systems. This is done within the frame of the Vienna Ab initio Simulation package (VASP)[13-14]. The projector-augmented plane wave (PAW)[15-16] describes the electron–ion interactions. The Monkhorst-Pack *k*-points of 1 × 1 × 3 are adopted to relax the geometrical structures. For all calculations, the symmetry is switched on and atomic relaxation is conduced until the total energy variation is less than 10^{-4} eV.

Moreover, the following equation is defined to compute the adsorption energy of the small gas molecules in the MOF system:

$$\Delta E_{ads} = E\,(MOF) + E\,(molecule) - E\,(MOF+molecule)$$

where E (MOF+molecule) and E(MOF) represent the total energies of the studied MOF systems with and without the gas molecules, and E (molecule) denotes the energy of the single gas molecule.

References

1 N. Wei, X. Zheng, H. Ou, P. Yu, Q. Lia and S. Feng.*New J. Chem.* 2019, *43*, 5603-5610.

2 M. Cai, L. Qin, L. You, Y. Yao, H. Wu, Z. Zhang, L. Zhang, X. Yin and J. Ni.*RSC Adv.* 2020, *10*, 36862-36872.

3 X. Y. Zhao, H. Yang, W. Y. Zhao, J. Wang and Q. S. Yang.*Dalton Trans.* 2021, *50* (4), 1300-1306.

4 E. Mateo-Martí, L. Welte, P. Amo-Ochoa, P. J. Sanz Miguel, J. Gómez-Herrero, J. A. Martín-Gago and F. Zamora.*Chem. Commun.* 2008, (8), 945-947.

5 P. Carmona.*Spectrochim. Acta, Part A* 1980, *36*, 705-712.
6 C. M. d. Silva, J. Ellena and R. C. G. Frem.*New J. Chem.* 2020, *44*, 10146-0152.
7 A. Karmakar, C. L. Oliver, S. Roy and L. Ohrstrom.*Dalton Trans.* 2015, *44* (22), 10156-10165.
8 X. Feng, X. L. Ling, L. Liu, H. L. Song, L. Y. Wang, S. W. Ng and B. Y. Su.*Dalton Trans.* 2013, *42* (28), 10292-10303.
9 J. Jiang, J. Zhang, P. Zhu, J. Li, X. Wang, D. Li, B. Liu, Q. Cui and H. Zhu.*RSC Adv.* 2016, *6*, 65031-65037.
10 J. P. Perdew, K. Burke and M. Ernzerhof.*Phys. Rev. Lett.* 1996, *77*, 3865-3868.
11 S. Grimme.*J Comput. Chem.* 2006, *27* (15), 1787-1799.
12 X. Wu, M. C. Vargas, S. Nayak, V. Lotrich and G. Scoles.*J. Chem. Phys.* 2001, *115* (19), 8748-8757.
13 G. Kresse and J. Hafner.*Phys. Rev. B Condens. Matter* 1994, *49* (20), 14251-14269.
14 G. Kresse and J. Hafner.*Phys. Rev. B Condens. Matter* 1993, *47* (1), 558-561.
15 P. E. Blochl.*Phys. Rev. B Condens. Matter* 1994, *50* (24), 17953-17979.
16 W. Li and D. Neuhauser.*Phys. Rev. B* 2020, *102* (19), 195118.